

Serpentine minerals from two areas of the Western Australian nickel belt

P. G. MOESKOPS

SUMMARY. Investigation of serpentine minerals from metaserpentinized ultramafic rocks in two Archaean greenstone belts, east of Kalgoorlie, has indicated that antigorite, exhibiting a very wide range of textures in thin section, is the dominant serpentine species; however, it is locally accompanied by relict lizardite. Chrysotile occurs both in late tectonic veins and as a present-day weathering product of relict olivine. Analytical data and structural formulae on seven serpentines, characterized independently by X-ray diffraction analysis, support the chemical differences between antigorite and chrysotile postulated by earlier workers.

INVESTIGATIONS were restricted to serpentine minerals from the Corsair metaserpentinites, immediately east of Kalgoorlie, and the metaserpentinized Bulong (ultramafic) Complex, about 30 km east of Kalgoorlie. The interpreted geological setting of these altered ultramafic intrusives (after Williams, 1969; modified by Moeskops, 1973) is indicated in fig. 1.

The Bulong Complex occurs within the regionally folded and metamorphosed acid volcanoclastic Gindalbie Formation. Detailed work on the Complex (Moeskops, 1973; Moeskops, in prep.) has indicated that its main concentration consists of an extensive, tightly folded, ultramafic-rich sill-zone. The structure consists of two opposite plunging synforms separated by an extensive saddle area as indicated in fig. 1. Most sills are composed of altered (metaserpentinized), layered, olivine-rich rocks but these are accompanied by fewer sills and rare dykes of altered pyroxenitic, gabbroic, dioritic, and granophyric rocks. Detailed work has also indicated that the Complex probably originated as a series of ultramafic and (fewer) basic magma pulses, which were introduced into near-horizontal country rocks; larger ultramafic pulses differentiated by convective-gravitational process to produce layered sills (composed mainly of olivine cumulates capped in part by thin zones of pyroxene and pyroxene-plagioclase cumulates), whereas smaller pulses simply froze to produce homogeneous 'quench texture' ultramafic sills, or underwent flowage differentiation, prior to crystallization, to produce zoned ultramafic sills. When igneous activity had virtually ceased, the Complex and its host rocks were regionally folded and metamorphosed.

The Corsair ultramafics consist of several conformable metaserpentinized olivine-rich sills, which reside within a narrow stratigraphic zone of the regionally folded and metamorphosed basic volcanoclastic Mulgabbie Formation, on the eastern side of the Lakewood Syncline, as indicated in fig. 1. Detailed work on these ultramafics (Moeskops, 1973; Moeskops and Nicholls, in prep.) has indicated that they originated as a series of olivine phenocryst-bearing ultramafic magma pulses, which were introduced into near-horizontal country rocks. During intrusion the sills underwent flowage differentiation prior to crystallization and were later deformed and altered (serpentinized and metamorphosed) along with their host rocks.

The Bulong and Corsair ultramafics are fundamentally different; the former are mainly altered layered cumulates composed originally of cumulus olivine plus accessory cumulus chromite, in association with variable amounts of intercumulus clinopyroxene, orthopyroxene, and plagioclase. The latter are not layered and consist mainly of altered olivine phenocrysts

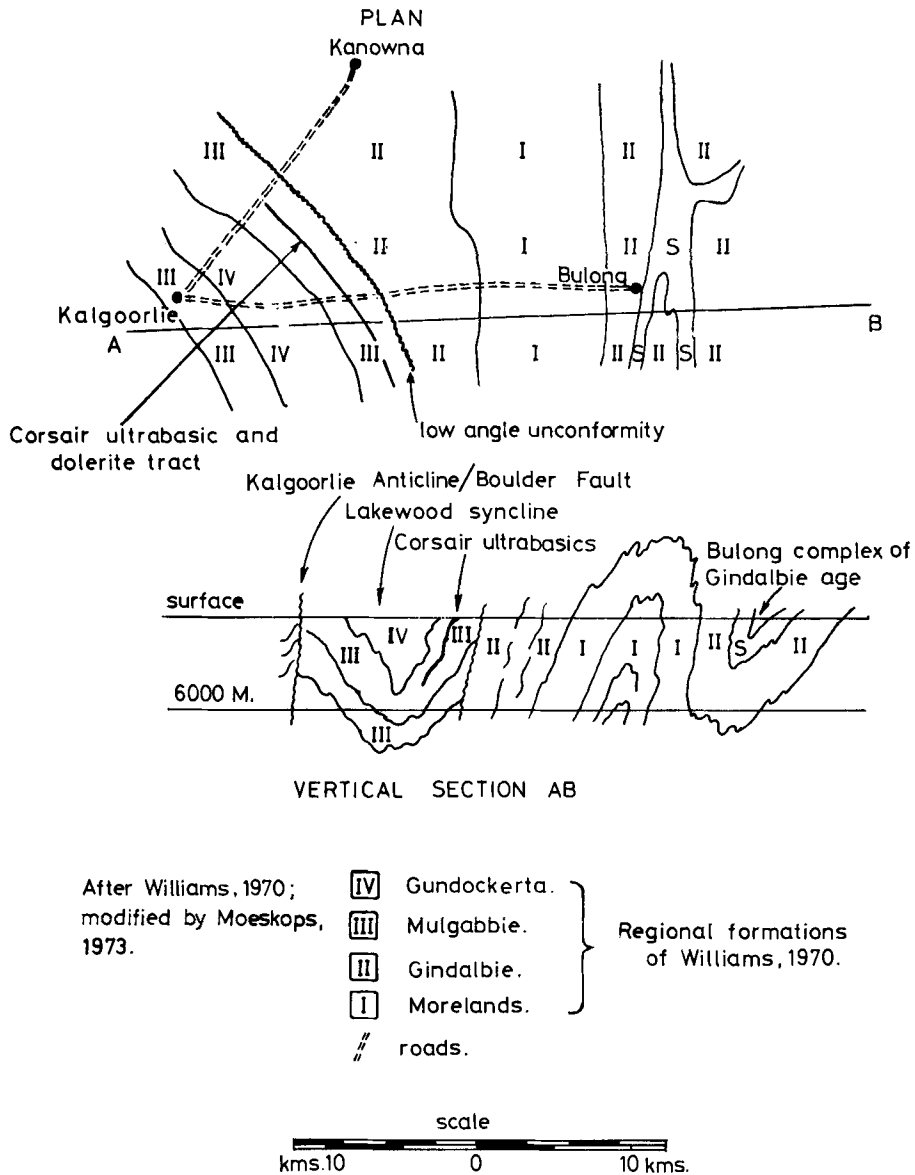


FIG. 1. Interpretive geological setting of the Bulong and Corsair ultramafics, east of Kalgoorlie, Western Australia (after Williams, 1970; modified by Moeskops, 1973).

plus accessory chromite phenocrysts in a 'quench texture' groundmass composed largely of clinopyroxene crystallites plus altered (chloritized) glass.

During regional metamorphism the country rocks about the Bulong Complex stabilized within the Middle Greenschist Facies whereas those about the Corsair ultrabasics stabilized within the Lower Greenschist Facies. Within the Lower Greenschist Facies pelitic rocks contain muscovite and chlorite, whereas within the Middle Greenschist Facies they contain biotite or chloritoid or both.

Terminology. 'Pseudomorphic' textures are common in the metaserpentinites of both areas. Using the nomenclature of Spry (1969) two main types of 'pseudomorphs' are evident: the first are *multicrystal pseudomorphs*, which consist of single crystals of olivine or pyroxene that have been replaced by a number of differently oriented crystals of a particular serpentine mineral (mainly antigorite); the second are *multi-phase/multicrystal pseudomorphs* consisting of single crystals of olivine or pyroxene that have been replaced by an aggregate of crystals of two or more serpentine minerals, usually antigorite plus lizardite. The terms 'alpha', 'gamma', and 'semi-isotropic' refer respectively to length fast, length slow, and low-birefringent ($\gamma-\alpha = 0.001-0.003$) serpentine variants, irrespective of species present. In the case of fibrous serpentine veins, those with fibres oriented roughly perpendicular to walls are referred to as 'cross-fibre' veins.

Textural features

Bulong Complex. Serpentinization of the Bulong Complex largely affected olivine-rich rocks; however, because the same rocks also suffered regional metamorphism, some primary serpentinization effects are probably no longer evident. Orthopyroxene and olivine were the minerals most susceptible to alteration; clinopyroxene was relatively resistant and other phases were largely unaffected.

The Bulong metaserpentinites are texturally similar to those described in the literature (e.g. Faust and Fahey, 1962; Lauder, 1965; Page, 1966; Coats, 1967; Spry, 1969; Basta and Kader, 1969; Williams, 1969; and Coleman and Keith, 1971; etc.) and are readily divisible into six main textural types:

Mesh texture metaserpentinites (nomenclature of Lauder, 1965). These predominate and are characterized by an abundance of net-like 'cords' (or veins), which are developed at various scales and which outline 'mesh' areas. 'Primary cords' are the most extensive and largest, and trace out 'primary mesh areas'. 'Secondary cords' emanate from primary cords and 'tertiary cords' emanate from secondary cords, and these respectively trace out 'secondary' and 'tertiary mesh areas' (fig. 2a). Cord patterns in relatively undeformed (massive) metaserpentinites are generally haphazard and mainly controlled by primary features such as cleavages, grain boundaries, and intragrain fractures. Cord patterns in weakly deformed metaserpentinites (fracture cleavage-bearing and weakly schistose variants) tend to be more regular and appear to be of deformational origin. Sub-parallel and pseudo-rectangular patterns predominate in these rocks although lensoid patterns are also seen. In detail, individual cords consist of simple or composite cross-fibre alpha serpentine veins with $\gamma-\alpha = 0.008-0.010$. In weakly altered rocks the mesh areas contain a high proportion of relict primary material whereas in totally altered rocks they consist largely of fibrous gamma serpentine ($\gamma-\alpha = 0.004-0.007$). In some sections, however, mesh areas consist of 'amorphous' (semi-isotropic) alpha serpentine ('serpophite' of Deer, Howie, and Zussman, 1967). Characteristic mesh textures are illustrated in figs. 2a, b.

Parallel vein texture metaserpentinites, which in outcrop appear weakly to moderately schistose, and which generally lack relict igneous textures, typically exhibit parallel vein texture in thin section. Pseudomorphs after olivine grains (but not the interstices between grains) are typically replaced by numerous closely spaced, sub-parallel, cross-fibre, alpha serpentine veinlets, which delineate schistosity. Pseudomorphs commonly appear highly distorted (i.e. squashed or stretched) and the interstitial serpentine consists variably of 'flakes', 'thorns', 'flames', 'plates', and 'needles' of gamma serpentine. These 'thorns', etc.

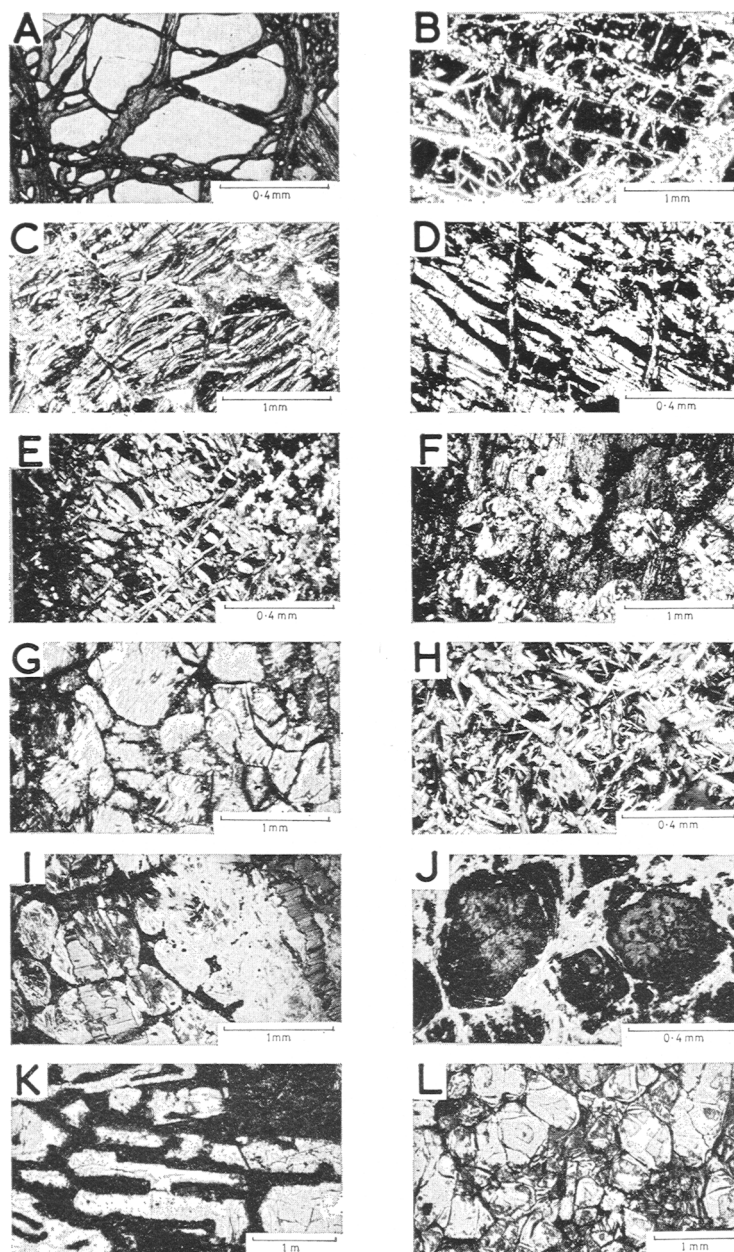


FIG. 2 (a): Olivine relics (light) cut by serpentine cords (dark) in partially metaserpentinized dunite. Polished section; plane polarized light. Sample BU649. (b): Pseudo-rectangular cord pattern in totally metaserpentinized dunite. Mesh areas (black) consist of semi-isotropic serpentine. Thin section; crossed polarizers. Sample BU611. (c): Typical parallel vein texture metaserpentinite. Note the distorted pseudomorphs after olivine grains. The veins consist of cross-fibre serpentine. Thin section; plane polarized light. Sample BU161. (d) and (e): Similar to (c); however, veins are leaf-like and disturbed by cross-cutting veinlets. Thin section; crossed polarizers. Sample BU162. (f) and (g): Pseudomorph texture metaserpentinites. Note that olivine and pyroxene have mainly been pseudomorphed by fibrous and flaky gamma serpentine. In photomicrograph (g) serpentine fibres tend to exhibit a common orientation throughout the section. Thin sections; crossed polarizers. Photomicrograph (f) is of sample BU178 and (g) is of sample BU108. (h): Fibro-lamellar, criss-cross pattern in schistose

often exhibit a marked (criss-cross) preferred orientation in two directions which are symmetrical about the direction of veining. Textural features are illustrated in figs. 2c–e.

'*Pseudomorph*' texture *metaserpentinites* are massive, apparently undeformed *metaserpentinites* that in thin section commonly exhibit near-perfect primary textural preservation (figs. 2f–g) strongly suggestive of constant volume serpentinization; however, such rocks invariably pass laterally or along strike (over distances of 3 to 20 cm) into rocks that exhibit less perfect textural preservation (described above and below) and in which a volume increase could have taken place.

Shear texture metaserpentinites. Samples from highly schistose zones in *metaserpentinites*, and from matrix areas in brecciated zones, in thin section totally lack textural evidence of original igneous origin and consist simply of fibrolamellar intergrowths of 'thorn', 'needle', and 'flame', etc. texture gamma serpentine. Thorns and needles, etc. often exhibit a marked preferred criss-cross pattern in two directions in the plane of schistosity, and in some sections they clearly spear and replace associated opaque phases. Characteristic 'shear texture' is illustrated in fig. 2h.

Asbestos-bearing metaserpentinites. Asbestos veins occur locally in parts of the Bulong Complex that have apparently suffered *high static stress* during deformation (mainly fold nose areas—see fig. 1). Veins consist of 'silky' cross-fibre gamma serpentine, are commonly associated with magnetite, and the surrounding material usually consists of fibrous and flaky gamma serpentine ($\gamma-\alpha = 0.008$). Characteristic textural features are shown in fig. 2i.

Non-fibrous, serpentine-rich veins. Late stage, cross-cutting (i.e. post tectonic, retrograde) serpentine-rich veins and veinlets abound throughout the Complex and typically contain minor amounts of associated talc, carbonate, chlorite, amphibole, magnetite, and sulphides. Such veins are commonly associated with small (2 to 15 mm sized), vesicular-looking patches of dark-green translucent serpentine, which appears semi-isotropic under crossed polarizers.

Although field and petrographic evidence imply that serpentinization in the Bulong Complex was largely syntectonic, it would be unwise to postulate one or more 'periods of serpentinization'. Serpentinization probably began at the late magmatic stage, continued throughout regional deformation and metamorphism (via innumerable increments of local deformation and ingress of water), and terminated with the development of the late stage (i.e. post-tectonic, retrograde) veins.

FIG. 2 (cont.)

metaserpentinite caused by thorns of gamma serpentine oriented in two main directions in the plane of schistosity. Thin section; crossed polarizers. Sample BU160. (i): Asbestos veins (cross-fibre gamma serpentine—antigorite) in *metaserpentinized* dunite. Note the veins 'cut through' and do not 'push apart' the pseudomorphs after olivine. Thin section; plane polarized light. Sample BU696. (j): Weathering serpentine (dark grey) after relict olivine. Material between the weathering serpentine patches consists of primary flaky gamma serpentine. Thin section; plane polarized light. Sample BU142. (k): Serpentine pseudomorphs (white) after skeletal olivine phenocrysts, embedded in a fine-grained groundmass composed of clinopyroxene crystallites and altered (chloritic) glass. Thin section; plane polarized light. Sample COR16. (l): Serpentine pseudomorphs after non-skeletal, equant and elongate olivine grains embedded in a fine-grained matrix of clinopyroxene and altered glass. Pseudomorphs contain kernels of relict olivine (light grey). Thin section; plane polarized light. Sample COR8.

Within the Complex there is clearly an implied inverse relationship between degree of textural preservation and intensity of deformation at the time of serpentinization, and the textural sequence,

pseudomorph or irregular mesh texture metaserpentinite→
 normal mesh texture metaserpentinite→
 parallel vein texture metaserpentinite→
 shear texture metaserpentinite,

is probably a reflection of increasing shearing stress. Olivine relics in near surface (i.e. weathered) samples are commonly replaced to varying degrees by iron-stained 'weathering serpentine' (fig. 2j). This weathering serpentine is apparently not uncommon in the Kalgoorlie region (Campbell, pers. comm., 1975).

Corsair ultramafics

Throughout the metaserpentinized Corsair sills olivine is largely replaced ('pseudomorphed') by gamma (i.e. length slow) serpentine, which exhibits characteristic fine 'mat' and 'hourglass' textures (Deer, Howie, and Zussman, 1967). Pseudomorphs from the cores of sills typically contain kernels of relict olivine (fig. 2l) and also appear non-skeletal, whereas those from the margins of sills appear skeletal and are devoid of olivine relics (fig. 2k). Textures in samples from deformed parts of the sills closely resemble those seen in deformed parts of the Bulong Complex (described above).

Analytical and X-ray data

Six chlorite-free rocks, displaying a broad spectrum of serpentinization textures, were chosen for pure serpentine-mineral separation. These and other samples were crushed and the 150–200-mesh fractions were sieved out, washed, and dried. Magnetite-bearing composite grains were then progressively removed, initially using a hand magnet and later using a Frantz Isodynamic Separator, set at progressively increasing current levels. Olivine and pyroxene relics, where present, were then separated from serpentine minerals using tetrabromethane. The nature and purity of the resultant serpentine separates was then determined by X-ray diffraction and by examining representative portions under the microscope in oil. X-ray runs, made using mechanical mixes of serpentine with chlorite, tremolite, olivine, pyroxene, and magnetite, indicated that proportions of these 'impurities' above 1.5 wt. % were readily detectable. The purity of serpentine separates selected for chemical analysis was estimated petrographically to be in excess of 99 % in all six cases. Because of the presence of chlorite in the Corsair metaserpentinites the chemical composition of the serpentine was determined by electron-probe micro analysis. Analysis of the six serpentine-rich separates was undertaken by the author using classical and semi-classical wet-chemical techniques; analytical and cation content data are listed in Table I. The serpentine species in these analysed, plus other separates, were identified by X-ray powder data using standard PDF index cards plus the data of Whitaker and Zussman (1956, pp. 111, 113, 117, and 121—includes charts), Hostetler *et al.* (1966, p. 82—includes charts), Page (1966, p. B105), Coats (1967, pp. 338–41, includes charts), and Basta and Kader (1969, p. 400).

Bulong Complex. X-ray study of the six above-mentioned separates, plus a further twenty-seven serpentine-rich separates, exhibiting a broad range of textures, clearly indicated that antigorite is the dominant serpentine species of the Bulong Complex. This mineral is characterized on X-ray diffraction charts by a strong and distinctive peak at 2.52 Å and by a pair of lines (the antigorite pair) at about 1.560 and 1.535 Å. The above mentioned late-stage,

cross-cutting green translucent veins and vesicular-looking patches were found to consist of a mixture of about 80 % clinochrysotile plus 20 % orthochrysotile, using the data of Whittaker and Zussman (1956). Weathering serpentinite (removed from several uncovered thin sections and X-rayed using a standard powder camera) was found to consist simply of clinochrysotile.

TABLE I. *Analyses and atomic ratios of serpentinite minerals from Bulong and Corsair, near Kalgoorlie, Western Australia*

Anal. No.	1	2	3	4	5	6	7
SiO ₂	43.4	43.1	42.7	41.5	42.3	41.0	43.1
Al ₂ O ₃	0.60	0.86	0.85	0.81	1.2	1.21	1.16
Cr ₂ O ₃	0.20	0.16	0.17	0.12	0.3	<0.01	0.05
Fe ₂ O ₃	0.18	0.24	0.28	0.46	—	2.31	0.58
FeO	2.15	2.13	2.01	2.06	6.1	0.58	1.18
MnO	0.11	0.09	0.10	0.11	0.1	0.03	0.08
NiO	0.12	0.14	0.14	0.15	0.1	0.13	0.12
MgO	40.2	40.6	41.0	42.1	36.5	41.6	40.6
H ₂ O ⁺	12.51	12.46	12.68	12.71	13.4	13.61	12.55
H ₂ O ⁻	0.24	0.18	0.12	0.12	..	0.32	0.18
Total	99.71	99.96	100.05	100.14	—	100.79	99.60
Atomic ratios to a basis of 9(O, OH)							
Si	2.035	2.018	1.995	1.944	1.989	1.895	2.015
Al ^{IV}	0.045	0.011	0.066	..
Al ^{VI}	0.034	0.048	0.047	—	0.056	—	0.064
Cr ³⁺	0.008	0.006	0.006	0.004	0.011	..	0.001
Fe ³⁺	0.006	0.009	0.010	0.016	..	0.081	0.020
Fe ²⁺	0.085	0.084	0.079	0.081	0.240	0.023	0.046
Mn	0.005	0.004	0.004	0.005	0.003	0.001	0.003
Ni	0.005	0.006	0.005	0.006	0.004	0.005	0.005
Mg	2.810	2.833	2.854	2.939	2.558	2.865	2.829
Σ	2.95	2.99	3.01	3.05	2.87	2.98	2.97
OH	3.914	3.892	3.951	3.971	4.204	4.195	3.915
Trace elements (ppm)							
Cu	10	10	10	15	10	25	15
Zn	35	30	40	35	40	45	40
Co	95	110	110	120	90	45	90

1. Pseudomorph texture serpentinite. Sample BU108.
2. Mesh texture serpentinite. Sample BU563.
3. Parallel vein texture serpentinite. Sample BU21.
4. Shear texture serpentinite. Sample BU279.
5. Typical Corsair mat-hourglass texture serpentinite. Sample COR16. H₂O by difference.
6. Late-stage, cross-cutting vein serpentinite. Sample BU637.
7. Asbestos vein serpentinite. Sample BU692.

Analyses 1 to 4, 6, and 7 were conducted using classical and semi-classical techniques; analysis 5 was conducted by electron-probe microanalysis. Independent X-ray diffraction analysis of the samples indicated that those listed as analyses 1 to 4 and 7 consist of antigorite, whereas analysis 5 consists of antigorite in association with lesser lizardite, and analysis 6 consists of a mixture of clinochrysotile plus lesser orthochrysotile.

Erratum: Anal. no. 5, delete trace element entries (10, 40, 90).

The last is characterized by a strong peak at about 2.45 Å and by a medium to weak band extending from 2.45 to about 2.59 Å. Peaks at 2.09 and 1.535 Å are also diagnostic. X-ray study of the Bulong Complex asbestos veins indicated that they are composed entirely of antigorite, and not of chrysotile as would be expected.

Corsair ultramafics. The serpentinite minerals in samples (one from near the core of a metaserpentinized sill; the other from near the margin) were identified by X-ray diffraction and the chemical composition of the serpentinite in one sample was determined by electron-probe

microanalysis (see Table I). The X-ray data indicated that the serpentinite from the core of the sill consists of a mixture of antigorite plus lesser lizardite and that the serpentinite from the margin of the sill consists only of antigorite.

Discussion and conclusions

Figs. 3a–f show Table I data plotted on to the variation diagrams of Whittaker and Wicks (1970), modified after Page (1966). Whittaker and Wicks 'acceptable' serpentinite analytical data, taken from Page (1966), are also plotted. These authors agree with Page's observation that, relative to lizardite and clinochrysotile, antigorite is enriched in SiO_2 and depleted in MgO and $\text{H}_2\text{O}+$. Furthermore, chrysotile contains H_2O in excess of that required by the ideal formula and antigorite exhibits the highest $\text{FeO}/(\text{FeO} + \text{Fe}_2\text{O}_3 + \text{Al}_2\text{O}_3)$ ratio. The data presented in this publication clearly conform with those conclusions.

In addition to plotting antigorite, lizardite, and clinochrysotile analytical data on to diagrams similar to figs. 3a–f, Page (1966) also conducted a statistical analysis of major oxide data and plotted (in terms of cations per 18 $\text{O} + \text{OH}$) the parameters $(\text{Fe}^{2+} + \text{Mg})$ vs. $(\text{Fe}^{3+} + \text{Al})$, $\Sigma(R^{3+} \text{ octahedral} - R^{3+} \text{ tetrahedral})$ vs. $\Sigma \text{ octahedral cations}$, and $\Sigma \text{ octahedral cations}$ vs. wt. % $\text{H}_2\text{O}+$. Page also plotted cation data on to the triangular diagram $\text{Al}-\text{Fe}^{3+}-\text{Fe}^{2+}$. Unfortunately many of the data were unacceptable, as pointed out by Whittaker and Wicks, and this led to an overinterpretation of the chemical differences between the three main serpentinite species. The main differences between the species are believed by this author to be accentuated in figs. 3a–f.

Data indicate that within the Bulong Complex antigorite is the dominant serpentinite mineral; however, post-tectonic serpentinite veins, and weathering serpentinite, after relict olivine, are composed of chrysotile. The presence of relict lizardite near the core of a sill at Corsair, and its apparent absence throughout the Bulong Complex, is in accordance with the observation that the Corsair sills suffered a slightly lower grade of regional metamorphism.

The most commonly recorded serpentinitization assemblage mentioned in the literature consists of lizardite–clinochrysotile–magnetite–(brucite); however, in the past studies have tended to be biased towards unmetamorphosed, or slightly metamorphosed, alpine-type, ultramafic rocks, which probably did not crystallize or even serpentinite *in situ*. The origin of the mineral antigorite (which has never been synthesized) is debatable; however, many recent authors (e.g. Green, 1961; Page, 1966; Černý, 1968) dismiss the notion that it is a 'stress mineral' (Harker, 1950), and consider that antigorite forms from, or in place of, low-temperature lizardite–clinochrysotile–(brucite) type assemblages during regional metamorphism. Serpentinitization temperatures, based on oxygen isotope fractionation ratios between coexisting serpentinite and magnetite (Wenner and Taylor, 1971), also support this suggestion. Their data indicate that alpine-type (i.e. unmetamorphosed) lizardite–clinochrysotile serpentinites formed at temperatures ranging between 85 and 115 °C, whereas antigorite-bearing (i.e. metamorphosed) serpentinites formed at temperatures ranging between 220 and 460 °C.

Extensive X-ray investigations (e.g. Hudson, Nesbitt, Purvis, Ramsden, Travis, Williams—pers. comm., 1971–4) have indicated that antigorite is the dominant serpentinite mineral of the Western Australian nickel belt; however, it is accompanied locally by lesser amounts of primary and secondary lizardite and clinochrysotile.

Weathering serpentinite (clinochrysotile), which locally replaces relict olivine in the Bulong Complex, is invariably associated with magnesite veins, and in diamond drill cores the proportions of weathering serpentinite and magnesite invariably decrease with increasing depth. The chemical reaction between (relict) forsteritic olivine and percolating groundwater can be

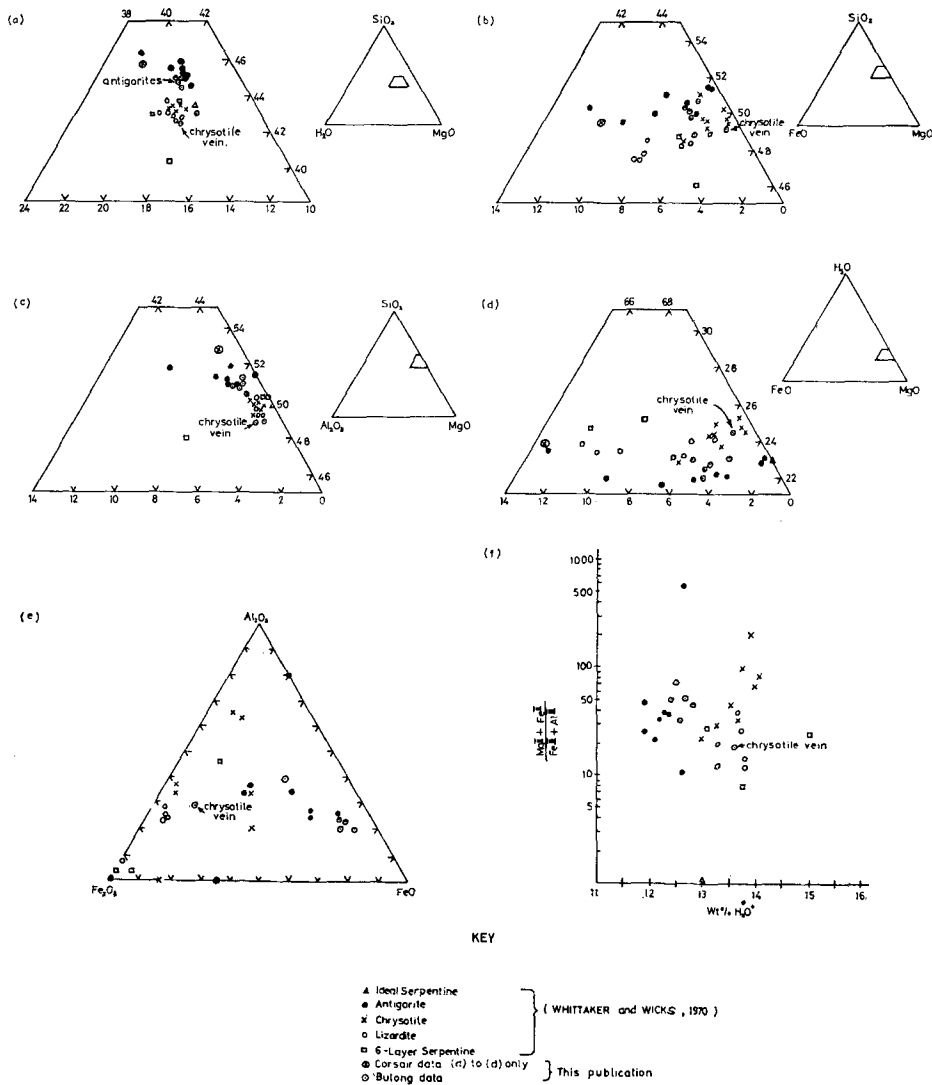


FIG. 3. Bulong and Corsair serpentine mineral analytical and cation content data, plotted onto six of the variation diagrams of Page (1966). The 'acceptable' data of Whittaker and Wicks (1970) are included for comparison.

written as: $2\text{Mg}_2\text{SiO}_4 + 3\text{H}_2\text{O} = \text{Mg}_3\text{Si}_2\text{O}_5(\text{OH})_4 + \text{Mg}^{2+} + 2\text{OH}^-$. A rise in pH is required by this equation and if CO_2 is present in the groundwater magnesite will precipitate. This present-day weathering serpentinization is similar to that described by Worst (1960), Barnes and Himmelberg (1967), Barnes and O'Neil (1969), and Campbell (1976) and is probably the main cause of magnesite veining, which is seen locally in ultramafic rocks throughout the Kalgoorlie region.

Acknowledgements. Data presented in this publication were collected in the course of Ph.D. research undertaken at London University. Research was financed by Australian Selection (Pty.) Ltd. and their financial assistance is gratefully acknowledged. The author also wishes to thank Dr. K. J. Henley, of Amdel, for checking the original manuscript.

REFERENCES

- Barnes (I. L.) and Himmelberg (G.), 1967. *Sci.* **156**, 830-2.
— and O'Neil (J. R.), 1969. *Bull. Geol. Soc. Amer.* **80**, 1947-60.
Basta (E. Z.) and Kader (Z. A.), 1969. *Mineral. Mag.* **37**, 394-408.
Campbell (I. H.), 1976. *Direct Evidence of Present-day Serpentinisation in the Jimberlana Intrusion, Western Australia* (in prep.).
Černý (P.), 1968. *Am. Mineral.* **53**, 1377-85.
Coats (C. J.), 1967. *Can. Mineral.* 322-47.
Coleman (R. G.) and Keith (T. E.), 1971. *J. Petrol.* **12**, 311-28.
Deer (W. A.), Howie (R. A.), and Zussman (J.), 1967. *The Rock Forming Minerals*. **4**. Longmans, London.
Faust (G. T.) and Fahey (J. J.), 1962. *U.S. Geol. Surv. Prof. Pap.* **384A**.
Green (D. H.), 1961. *Geol. Mag.* **98**, 1-26.
Harker (A.), 1950. *Metamorphism*. Methuen, London.
Hostetler (B. P.), Coleman (R. G.), Mumpton (F. A.), and Evans (B. W.), 1966. *Am. Mineral.* **51**, 175-98.
Lauder (W. R.), 1965. *N.Z. J. Geol. Geophys.* **8**, 475-504.
Moeskops (P. G.), 1973. *The Bulong Serpentinite and Environments of Nickel Mineralisation near Kalgoorlie, Western Australia*. Unpub. Lond. Univ. Ph.D. thesis.
— and Nicholls (I. A.), 1976. *The Corsair Metaserpentinites, near Kalgoorlie, Western Australia* (in prep.).
Page (N. J.), 1966. *The Mineralogy and Chemistry of the Serpentine Group Minerals and the Serpentinisation Process*. Unpub. Berkeley, Ph.D. thesis.
Spry (A.), 1969. *Metamorphic Textures*. Oxford, Pergamon Press.
Wenner (D. B.) and Taylor (H. P.), 1971. *Contr. Mineral. Petrol.* **32**, 165-85.
Whittaker (E. J. W.) and Wicks (F. J.), 1970. *Am. Mineral.* **55**, 1025-47.
— and Zussman (J.), 1956. *Mineral. Mag.* **31**, 107-26.
Williams (I. R.), 1969. *Explanatory Notes on the Kurnalpi 1:250,000 Geological Sheet: West. Aust. Geol. Surv. Rec.* (unpublished).
Worst (B. G.), 1960. *Bull. South. Rhodesian Geol. Surv.* **47**.

[Manuscript received 5 April 1976; revised 20 August 1976]